Development of Novel Tetravalent Anti-CD20 Antibodies with Potent Antitumor Activity

Bohua Li,[1,2] Shu Shi,[1] Weizhu Qian,[1,2] Lei Zhao,[1] Dapeng Zhang,[1] Sheng Hou,[1,2] Lei Zheng,[1] Jianxin Dai,[1] Jian Zhao,[1] Hao Wang,[1,2] and Yajun Guo[1,2]

[1]International Joint Cancer Institute, Second Military Medical University and [2]Shanghai Center for Cell Engineering and Antibody, Shanghai, People's Republic of China

Abstract

Despite the effectiveness of the anti-CD20 monoclonal antibody (mAb) Rituximab (C2B8) in the treatment of B-cell lymphoma, its efficacy remains variable and often modest. It seems likely that a combination of multiple mechanisms, such as complement-dependent cytotoxicity (CDC) and apoptotic signaling, underlies the therapeutic success of anti-CD20 mAbs. Unfortunately, all the current anti-CD20 mAbs effective in CDC are relatively inactive in signaling cell death and vice versa. In this study, we developed two genetically engineered tetravalent antibodies (TetraMcAb) respectively derived from the anti-CD20 mAbs C2B8 and 2F2. TetraMcAbs, with a molecular mass only 25 kDa higher than native divalent antibodies (DiMcAb), were shown not only to be as effective in mediating CDC and antibody-dependent cellular cytotoxicity against B-lymphoma cells as DiMcAbs but also to have antiproliferative and apoptosis-inducing activity markedly superior to that of DiMcAbs. Interestingly, whereas 2F2 and C2B8 were equally effective in inducing cell growth arrest and apoptosis, the functions of their tetravalent versions, 2F2(ScFvHL)$_4$-Fc and C2B8(ScFvHL)$_4$-Fc, were significantly different. 2F2(ScFvHL)$_4$-Fc exhibited exceptionally more potent antiproliferative and apoptosis-inducing activity than that of C2B8(ScFvHL)$_4$-Fc. Immunotherapeutic studies further showed that 2F2(ScFvHL)$_4$-Fc was far more effective in prolonging the survival of severe combined immunodeficient mice bearing systemic Daudi or Raji tumors than C2B8, 2F2, and C2B8(ScFvHL)$_4$-Fc, suggesting that it might be a promising therapeutic agent for B-cell lymphoma. [Cancer Res 2008;68(7):2400–8]

Introduction

The CD20 antigen is present on >90% of B-cell lymphomas and is neither shed nor internalized after antibody binding, making it an effective target for immunotherapeutic removal of malignant B cells (1–3). The mouse/human chimeric anti-CD20 antibody, Rituximab (C2B8), is the first therapeutic monoclonal antibody (mAb) approved for the treatment of relapsed/refractory low-grade or follicular B-cell non–Hodgkin's lymphomas (NHL; refs. 4–6). Despite the effectiveness of Rituximab, only 48% of patients respond to the treatment and complete responses are <10%. In addition, a significant number of patients have progressive disease during antibody therapy (7, 8). There is an urgent need to develop more effective anti-CD20 molecules to further improve the efficacy of antibody therapy for B-cell lymphoma (9–14).

The successful improvement of therapeutic efficacy relies in large part on an understanding of the mechanism by which Rituximab functions. Previous studies have suggested that several mechanisms might be involved in providing therapeutic efficacy, including complement-dependent cytotoxicity (CDC), antibody-dependent cellular cytotoxicity (ADCC), and the induction of cell growth arrest and apoptosis. The relative contributions of these different mechanisms of action are still a matter of debate. However, it is becoming clear that the multiple potential mechanisms are not independent and mutually exclusive but are likely to be interactive and potentially cooperative components of Rituximab-mediated therapy. In addition, select mechanisms of action may vary in importance among different CD20-positive lymphoproliferative disorders (9). Therefore, it is rational to conclude that the patients unresponsive to Rituximab may be effectively treated by other versions of anti-CD20 antibodies with different biological activities. Anti-CD20 mAbs are usually defined as either type I or II, based on their efficacy in various *in vitro* assays (15). Type I mAbs (Rituximab and most anti-CD20 mAb) are potent in CDC assays and less effective in induction of apoptosis, whereas type II mAbs (B1 and 11B8) are effective in inducing apoptosis but ineffective in CDC (13, 16). In addition to Rituximab, B1 has also been approved for treatment of NHL as an I^{131} conjugate. Interestingly, even as a "naked" mAb, B1 is capable of inducing objective responses in NHL patients, including a number of complete responses (15, 17). In fact, preclinical data also suggested that the naked B1 was as effective as the I^{131}-labeled compound (18). Due to the significantly different activities of the two types of anti-CD20 antibodies, the patients who are resistant to type I antibodies may benefit from treatment with type II antibodies and vice versa. Thus, an anti-CD20 antibody, which is not only effective in CDC but also potent in inducing apoptosis, might be able to kill CD20-positive lymphoma cells more effectively. Unfortunately, all the current anti-CD20 mAbs effective in CDC are relatively inactive at signaling cell death.

In the present study, we have developed two genetically engineered tetravalent antibodies (TetraMcAb) respectively derived from two type I anti-CD20 mAbs, C2B8 and 2F2. 2F2 is a fully human anti-CD20 mAb, which is significantly more potent than C2B8 in CDC (13). The *in vitro* and *in vivo* antitumor activity of TetraMcAbs were examined and compared with the parental divalent IgG1, κ antibodies (DiMcAb). 2F2(ScFvHL)$_4$-Fc, the TetraMcAb derived from 2F2, was shown not only to be as effective in mediating CDC and ADCC as 2F2 but also to have potent antiproliferative and apoptosis-inducing activity significantly superior to that of 2F2, C2B8, and the C2B8-derived TetraMcAb. Results from immunotherapeutic studies further revealed that

Note: B. Li and S. Shi contributed equally to this work as first authors.

Requests for reprints: Yajun Guo, International Joint Cancer Institute, Second Military Medical University, 800 Xiang Yin Road, Shanghai 200433, People's Republic of China. Phone: 86-21-25070241; Fax: 86-21-25074349; E-mail: yjguo@smmu.edu.cn.

doi:10.1158/0008-5472.CAN-07-6663

2F2(ScFvHL)$_4$-Fc was far more effective in prolonging the survival of severe combined immunodeficient (SCID) mice bearing systemic human B-cell lymphomas than the other three anti-CD20 mAbs, suggesting that it might be a promising therapeutic agent for the treatment of B-cell lymphoma.

Materials and Methods

Cell lines, antibodies, and animals. Two human Burkitt lymphoma cell lines, Raji and Daudi, and one human T-lymphoma cell line, Jurkat, were obtained from the American Type Culture Collection (ATCC). Rituximab (C2B8) and the anti-HER2 humanized antibody Trastuzumab (anti-HER2) were purchased from Roche Ltd. C2B8 and anti-HER2 were labeled with FITC to produce FITC-conjugated antibodies C2B8-FITC and anti-HER2–FITC, respectively. The Chinese hamster ovary (CHO)-K1 cell line and human leukemia cell line U937 were purchased from ATCC. CHO-K1 cell line highly expressing the human CD20 cell surface antigen (CHO-CD20) was established and maintained in our laboratory. Eight-wk-old female ICR mice and BALB/c SCID mice were obtained from the Planned Parenthood Research Institute. All animals in this study were housed in pathogen-free conditions and were treated in accordance with guideline of the Committee on Animals of the Second Military Medical University.

Construction of expression vectors for anti-CD20 TetraMcAbs. The heavy and light chain variable region genes of C2B8 (Fig. 1*A*; ref. 19) or 2F2 (Fig. 1*A*; ref. 13) were synthesized by Sangon Biological Engineering Technology Company. The C2B8 heavy chain variable region gene was fused to the 5′ end of its light chain variable region gene via a linker sequence $(Gly_4Ser)_3$ to generate the C2B8 single chain antibody gene C2B8(ScFvHL). To construct the expression vector for the C2B8-derived TetraMcAb, C2B8(ScFvHL)$_4$-Fc (Fig. 1*A*), two identical C2B8(ScFvHL) genes were linked in tandem via a short sequence coding for a flexible peptide linker (ASTGS; refs. 20, 21) to generate the C2B8(ScFvHL)$_2$ gene. Then, the C2B8(ScFvHL)$_2$ gene was genetically fused in frame to the 5′ terminus of the human IgG1 Fc (hinge, CH2, and CH3 domains) gene, and the resulting C2B8(ScFvHL)$_2$-hinge-CH2-CH3 gene was cloned into the pcDNA3.1(+) vector (Invitrogen), yielding the expression vector for C2B8(ScFvHL)$_4$-Fc. Likewise, the expression vector for generating the 2F2-derived TetraMcAb, 2F2(ScFvHL)$_4$-Fc (Fig. 1*A*), was obtained using the same method as described above, except that the C2B8(ScFvHL) gene was replaced with the 2F2(ScFvHL) gene. The light and heavy chain expression vectors for 2F2 were constructed using the same method as described in our previous report (22).

Expression and purification of anti-CD20 antibodies. The 2F2 mAb was expressed and purified using the identical procedures described previously (22). For the expression of C2B8(ScFvHL)$_4$-Fc and 2F2(ScFvHL)$_4$-Fc,

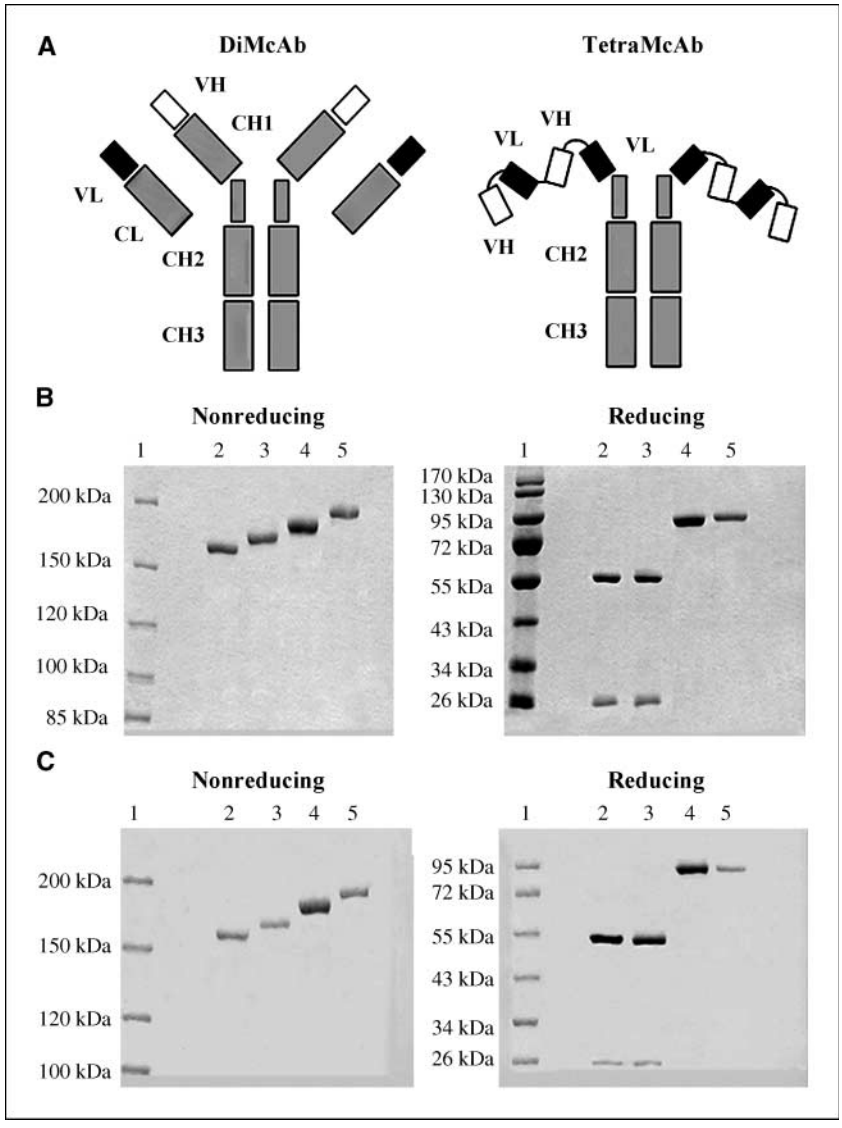

Figure 1. Structure and size comparison of TetraMcAb and DiMcAb. *A,* schematic representation of the structures of DiMcAb (C2B8 or 2F2) and TetraMcAb [C2B8(ScFvHL)$_4$-Fc or 2F2(ScFvHL)$_4$-Fc]. *B,* SDS-PAGE analysis of purified anti-CD20 mAbs under nonreducing and reducing conditions. *Lane 1,* molecular weight protein markers; *lane 2,* C2B8; *lane 3,* 2F2; *lane 4,* C2B8(ScFvHL)$_4$-Fc; *lane 5,* 2F2(ScFvHL)$_4$-Fc. *C,* Western blot analysis of purified anti-CD20 mAbs separated by SDS-PAGE. *Lane 1,* molecular weight protein markers; *lane 2,* C2B8; *lane 3,* 2F2; *lane 4,* C2B8(ScFvHL)$_4$Fc; *lane 5,* 2F2(ScFvHL)$_4$Fc.

their expression vectors were respectively transfected into CHO-K1 cells using Lipofectamine 2000 reagent (Invitrogen). After transfection, the stable transfectants were isolated by limiting dilution in the presence of 500 μg/mL G418. The cell clones producing the highest amount of TetraMcAbs were selected and grown in serum-free medium. Finally, TetraMcAbs were purified by affinity chromatography on Protein A-Sepharose (Amersham Biosciences) from the serum-free culture supernatants.

SDS-PAGE and Western blot. The purified proteins were analyzed on 6% SDS-PAGE under nonreducing conditions and on 12% SDS-PAGE under reducing conditions, followed by Coomassie Brilliant Blue staining. For Western blot analysis, proteins were separated by SDS-PAGE under nonreducing and reducing conditions and then electrophoretically transferred onto polyvinylidine difluoride (PVDF) membranes (Amersham Biosciences). After protein transfer, the PVDF membranes were treated with the blocking buffer followed by incubation with horseradish peroxidase–conjugated goat anti-human IgG (H+L; Zymed). Finally, the bands were visualized by 3,3′-diaminobenzidine (Sigma) as a peroxidase substrate.

Binding of TetraMcAbs to Raji cells. Flow cytometry analysis (FCM) was performed to determine the binding of TetraMcAbs to Raji cells using a FACScan flow cytometer (Becton Dickinson). Briefly, Raji cells at 1×10^6 cells/mL were incubated with different concentrations of FITC-labeled recombinant antibodies for 1 h at 4°C. Then, the cells were washed and analyzed by FCM.

Competitive binding assay. Raji cells at 1×10^6 cells/mL were incubated with a subsaturating concentration of the FITC-conjugated C2B8 or 2F2 (C2B8-FITC or 2F2-FITC) and increasing concentrations of competing antibodies for 1 h at 4°C. The cells were then washed and analyzed by FCM. The IC_{50} values of competitors were calculated using a four-variable algorithm.

Binding of human complement subcomponent C1q to TetraMcAbs. Raji cells at 1×10^6 cells/mL were incubated with 2 μg/mL of anti-CD20 recombinant antibodies at 37°C for 15 min. After washing, the cells were incubated with normal human serum (NHS; 1% vol/vol) for 15 min at 37°C. The cells were washed again and then incubated with FITC-labeled sheep anti-human Clq mAb (Serotec) for 30 min at 4°C. At the end of the incubation, the cells were washed and analyzed by FCM.

Binding of TetraMcAbs to U937 cells. FcR binding competition assay was performed as described in our previous report (22). Briefly, U937 cells bearing both FcRI and FcRIII (23, 24) were incubated with subsaturated concentrations of anti-HER2–FITC and increasing concentrations of purified anti-CD20 mAbs for 1 h at 4°C. After incubation, the cells were washed and analyzed by FCM.

Dissociation rate of TetraMcAbs. To determine the dissociation rate of TetraMcAbs from Raji cells, the cells were incubated with saturating FITC-labeled TetraMcAbs (10 μg/mL) at 37°C for 1 h, washed twice, and resuspended in complete medium. After different time intervals, the samples were taken, washed, and analyzed by FCM to determine the percentage of the remaining cells that were still stained.

Cytotoxicity assays. CDC and ADCC activities of TetraMcAbs were measured by lactate dehydrogenase (LDH)-releasing assay using the CytoTox 96 non-Radioactive Cytotoxicity Assay kit (Promega) according to the manufacturer's instructions. Briefly, the cells were incubated with TetraMcAbs for 1 h in phenol red-free DMEM culture medium in a 5% CO_2 incubator at 37°C, followed by the addition of either NHS (10% vol/vol) as a source of complement (for CDC assay) or human peripheral blood mononuclear cells (PBMC) as effector cells (effector to target, 50:1 for ADCC assay). After an additional incubation for 4 h at 37°C, the cell lysis was determined by measuring the amount of LDH released into the culture supernatant. Maximum LDH release was determined by lysis in 0.2% Triton X-100. Percentage of specific lysis was calculated according to the following formula: % lysis = [experimental release − spontaneous release]/[maximum release − spontaneous release] × 100.

Apoptosis assay. The cells were incubated with different concentrations of anti-CD20 mAbs at 37°C for 18 h. After washing, cells were treated with Annexin V-FITC (BD Biosciences PharMingen), washed again, and analyzed by FCM. $F(ab')_2$ fragment of goat anti-human IgM (anti-IgM; Jackson ImmunoResearch Laboratories) was used as a positive control for the induction of apoptosis.

[^{3}H]thymidine assay. Daudi or Raji cells at 5×10^5 cells/mL were incubated with different concentrations of anti-CD20 mAbs in 96-well plates at 37°C for 24 h. Then, [^{3}H]thymidine was added at 1 μCi/well. After an additional 12-h incubation, the cells were harvested and [^{3}H]thymidine incorporation was measured in a liquid scintillation counter.

Cell growth inhibition assay. Raji, Daudi, or Jurkat cells at 2×10^5 cells/mL were incubated with different concentrations of anti-CD20 antibodies in complete medium at 37°C, 5% CO_2. Viable cells were counted daily by trypan blue exclusion for 5 d, and the cell growth curves were determined. On the 5th d, the cell growth inhibition was evaluated by the 3-(4,5-dimethylthiazol-2-yl)-2,5-diphenyltetrazolium bromide (MTT) assay described previously (25). MTT was obtained from Sigma. The percentage of cell growth inhibition was calculated according to the following formula: Inhibition (%) = $[(A492_{\text{mAb-untreated cells}} - A492_{\text{mAb-treated cells}})/(A492_{\text{mAb-untreated cells}} - A492_{\text{culture medium}}) \times 100$.

Pharmacokinetic analysis. Groups of 8-wk-old female ICR mice were injected with 50 μg of mAbs via the tail vein. Blood samples were taken every other day by retro-orbital bleeding and collected in tubes coated with heparin to prevent clotting. Four mice were used for every time, and each mouse was bled only once. After centrifugation to remove the cells, the plasma samples were stored at −80°C until analysis. Plasma concentrations of mAbs were determined using the same method described previously (26). Briefly, the plasma samples were incubated with CHO-CD20 cells, and then, the bound recombinant antibodies were detected with FITC-goat anti-human IgG(H+L) by FCM. Finally, the pharmacokinetic variables were calculated using a noncompartmental analysis.

Immunotherapy. Groups of 10 8-wk-old female SCID mice were injected via the tail vein with 3.5×10^6 Raji or Daudi cells on day 0, followed 5 d later by the i.v. injection of different doses of mAbs. The mice were observed daily and euthanized at the onset of hind leg paralysis.

Statistical analysis. Statistical analysis was performed by Student's unpaired *t* test to identify significant differences unless otherwise indicated. Differences were considered significant at a P value of <0.05.

Results

Construction and characterization of TetraMcAbs. The purity and the molecular weight of the purified anti-CD20 mAbs were determined by SDS-PAGE (Fig. 1*B*). Under reducing conditions, 2F2 yielded two protein bands with molecular mass of ~55 kDa (heavy chain) and ~26 kDa (light chain), whereas the 2F2(ScFvHL)$_4$-Fc migrated as a single band of ~93 kDa, corresponding approximately to the calculated molecular mass of the monomeric polypeptides. SDS-PAGE analysis under nonreducing conditions showed a single band of ~162 kDa for 2F2 and a ~186 kDa band for 2F2(ScFvHL)$_4$-Fc. C2B8 and C2B8(ScFvHL)$_4$-Fc displayed a similar pattern of protein bands to that observed by SDS-PAGE analysis of 2F2 and 2F2(ScFvHL)$_4$-Fc, respectively. These results indicated that 2F2(ScFvHL)$_4$-Fc or C2B8(ScFvHL)$_4$-Fc formed disulfide-linked dimers, and that 2F2 or C2B8 was composed of two light and two heavy chains, held together with disulfide bonds. The identity of the purified TetraMcAbs was further confirmed by Western blot using polyclonal antibodies against human IgG (Fig. 1*C*). These results show that the molecular mass of TetraMcAb is only ~25 kDa higher than that of its DiMcAb, although it contains four antigen-binding sites.

The binding of anti-CD20 mAbs to Raji cells was assessed in antigen-binding assays. As shown in Fig. 2*AI*, 2F2 and C2B8 gave similar binding curves, which was in agreement with that reported previously (13). Both of the two TetraMcAbs bound to Raji cells with the antigen-binding activity similar to that of their respective DiMcAbs. In the competitive binding assays, TetraMcAbs effectively

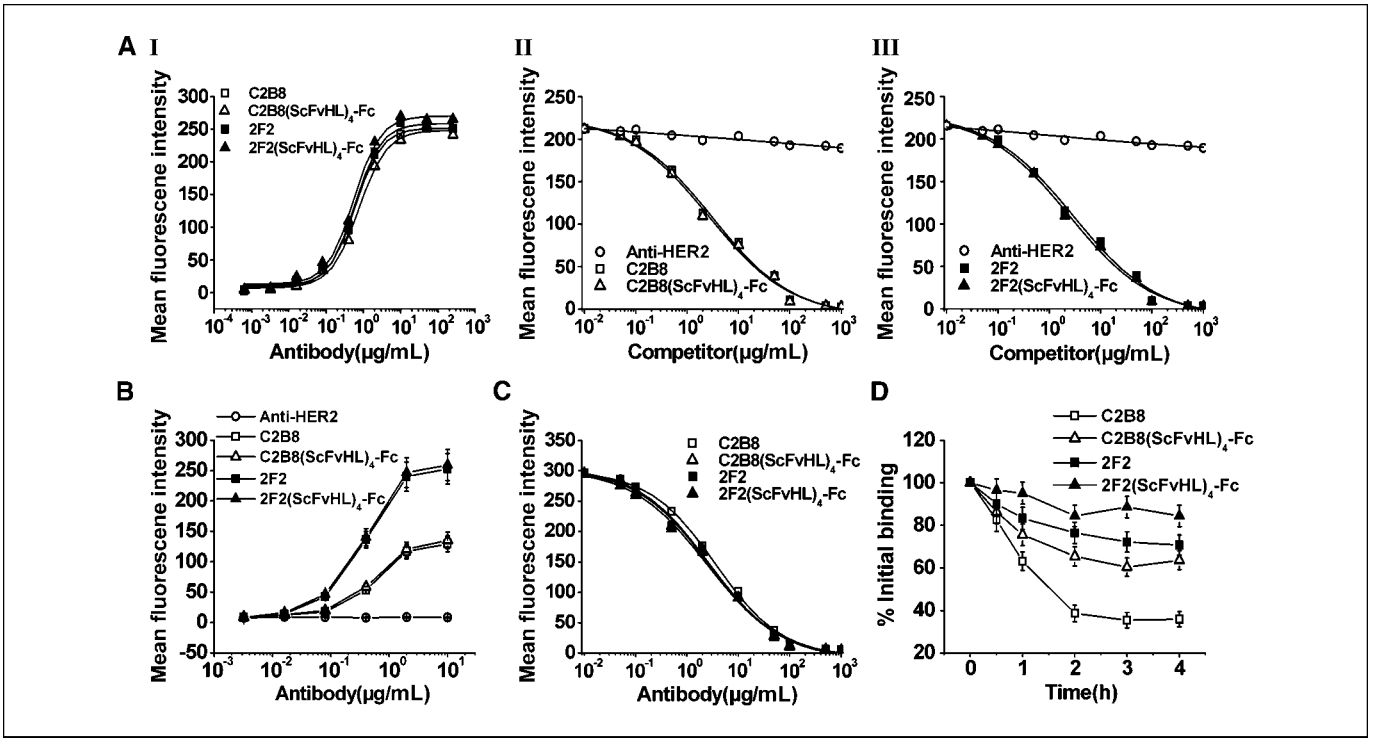

Figure 2. Characterization of TetraMcAbs. *A,* antigen binding activity of TetraMcAbs. *I,* antigen binding assays for TetraMcAbs. Raji cells were incubated with different concentrations of C2B8-FITC, 2F2-FITC, C2B8(ScFvHL)$_4$-Fc-FITC, or 2F2(ScFvHL)$_4$-Fc-FITC for 1 h at 4°C. Then, the cells were washed and analyzed by FCM. *Points,* mean of three independent experiments. *II* to *III,* competitive binding assay. Binding of C2B8-FITC (*II*) or 2F2-FITC (*III*) to Raji cells in the presence of increasing concentrations of competitor antibodies. Anti-HER2 is a humanized anti-HER2 antibody that does not compete with anti-CD20 antibodies. *Points,* mean of three independent experiments. *B,* C1q binding activity of anti-CD20 mAbs. Raji cells were incubated with 2 μg/mL of C2B8, 2F2, C2B8(ScFvHL)$_4$-Fc, or 2F2(ScFvHL)$_4$-Fc for 15 min at 37°C, followed by the addition of NHS (1% vol/vol) as a source of complement and incubation at 37°C for 15 min. Then, deposition of C1q was assessed by FCM after incubation of the cells with FITC-labeled antibody against C1q. Anti-HER2 is a negative control antibody. *Points,* mean (n = 6); *bars,* SD. *C,* binding of anti-CD20 mAbs to U937 cells. Human U937 cells were incubated with subsaturated concentrations of anti-HER2–FITC and increasing concentrations of C2B8, 2F2, C2B8(ScFvHL)$_4$-Fc, or 2F2(ScFvHL)$_4$-Fc for 1 h. Then, the cells were washed and analyzed by FCM. *Points,* mean of three independent experiments. *D,* dissociation of FITC–anti-CD20 mAbs from Raji cells. Cells were incubated with FITC-labeled anti-CD20 mAbs (10 μg/mL) at 37°C for 1 h, washed twice, and resuspended in complete medium. Samples of cells were taken at time 0, 0.5, 1, 2, 3, and 4 h and then washed and analyzed by FCM. *Points,* percentage of initial binding at time 0 and the mean (n = 3); *bars,* SD.

competed with DiMcAbs for binding to Raji cells (Fig. 2*AII* and *III*). The avidity (mean $IC_{50} \pm$ SD) of 2F2(ScFvHL)$_4$-Fc and C2B8(ScFvLH)$_4$-Fc (2.51 ± 0.21 and 2.67 ± 0.28 μg/mL) was respectively similar to that of 2F2 and C2B8 (2.69 ± 0.35 and 2.75 ± 0.29 μg/mL), suggesting that TetraMcAbs possessed affinity and specificity similar to that of their bivalent counterparts.

We next investigated the abilities of TetraMcAbs to fix C1q, the first component of the complement cascade. The results (Fig. 2*B*) indicated that both of the two TetraMcAbs effectively bound C1q, and the amount of C1q they bound was about equal to that of their respective DiMcAbs, indicating that TetraMcAb retained the capacity to fix C1q and thus had the potential to activate complement.

The ability of TetraMcAb and DiMcAb to bind to FcR on U937 cells was also compared. As shown in Fig. 2*C*, all of the four mAbs bound to FcR with a similar binding affinity. These results suggested that these tetravalent antibody constructs might be able to mediate ADCC with human FcR–bearing effector cells.

Dissociation experiments were performed by means of a direct immunofluorescence assay in which Raji cells were saturated with FITC-labeled mAbs and the stained cells were quantified after different incubation times. As shown in Fig. 2*D*, C2B8 dissociated much more rapidly than 2F2, which is consistent with the results reported by Teeling et al (13). The two TetraMcAbs had a significantly slower off rate than their respective DiMcAbs did, indicating that these tetravalent constructs engaged more than two of its binding sites and were able to persist for longer time on the cell surface.

CDC activity of TetraMAbs. To explore the capacity of TetraMcAbs to mediate CDC, two $CD20^+$ human lymphoma cell lines, Daudi and Raji, were used for this experiment. The results summarized in Fig. 3 clearly showed that 2F2 lysed Daudi cells much more effectively than did C2B8, and that the two TetraMcAbs were able to mediate CDC against Daudi cells comparably to their respective DiMcAbs. The similar results (Fig. 3) were obtained with Raji cells, which are more resistant to CDC than Daudi cells.

ADCC activity of TetraMcAbs. The anti-CD20 mAbs were compared for their ability to lyse $CD20^+$ cells in the presence of human PBMCs. The results (Fig. 3) indicated that C2B8, 2F2, 2F2(ScFvHL)$_4$-Fc, and C2B8(ScFvHL)$_4$-Fc were equally effective in inducing ADCC against Daudi or Raji cells in a dose-dependent manner. All of the four mAbs were unable to mediate ADCC activity in the $CD20^-$ cell line Jurkat (data not shown).

Induction of apoptosis in $CD20^+$ cell lines by TetraMAbs. Induction of apoptosis was evaluated by FITC-Annexin V assays in Daudi and Raji cells. As shown in Fig. 4*A*, both of the two native DiMcAbs, C2B8 and 2F2, triggered a low level of apoptosis (<10%) in the two cell lines at concentrations even up to 10 μg/mL.

However, apoptosis induced by TetraMcAbs was substantially higher than that induced by DiMcAbs ($P < 0.05$ for TetraMcAbs compared with their respective DiMcAbs at concentrations of 0.4, 2, and 10 μg/mL). Interestingly, although C2B8 and 2F2 caused the same level of apoptosis of Daudi cells, their tetravalent antibodies seemed to induce significantly different amount of apoptotic cells at concentrations of 0.4 μg/mL and higher ($P < 0.05$). 2F2(ScFvHL)$_4$-Fc was a strong inducer of apoptosis, resulting in ~30% apoptosis of Daudi cells at the concentrations of 2 and 10 μg/mL, whereas C2B8(ScFvHL)$_4$-Fc was much less potent in inducing apoptosis, and the maximum percentage of apoptotic cells was only ~19% when treating Daudi cells with C2B8 (ScFvHL)$_4$-Fc at all concentrations used in this experiment (Fig. 4*A*). The markedly greater level of apoptosis of Raji cells was also observed with 2F2(ScFvHL)$_4$-Fc than with C2B8(ScFvHL)$_4$-Fc (Fig. 4*A*).

Inhibition of [^{3}H]thymidine incorporation. The antiproliferative activity of anti-CD20 mAbs was determined by means of a [^{3}H]thymidine incorporation assay on Daudi and Raji cells. The results (Fig. 4*B*) showed that C2B8 and 2F2 had similar weak inhibitory effect on [^{3}H]thymidine incorporation in the two cell lines. In contrast, both of the two TetraMcAbs exhibited very potent antiproliferative activity against Daudi and Raji cells. Like the apoptosis-inducing activity, the antiproliferative activity of the two anti-CD20 tetravalent antibodies was also significantly different [$P < 0.05$ for 2F2(ScFvHL)$_4$-Fc compared with C2B8(ScFvHL)$_4$-Fc at concentrations of 0.4, 2 and 10 μg/mL]. 2F2(ScFvHL)$_4$-Fc was shown to inhibit the proliferation of lymphoma cells much more effectively than C2B8(ScFvHL)$_4$-Fc (Fig. 4*B*).

Growth inhibition by TetraMAbs. Daudi and Raji cells were cultured with anti-CD20 mAbs for 5 days. The number of viable cells was counted daily, and the cell growth rates were monitored. As depicted in Fig. 4*C*, the growth rate of cells treated with either of the four anti-CD20 antibodies [C2B8, 2F2, C2B8(ScFvHL)$_4$-Fc, or 2F2(ScFvHL)$_4$-Fc] was much lower than that of the anti-HER2 control antibody–treated cells. Daudi and Raji cells treated with TetraMcAbs grew significantly slowly than those treated with DiMcAbs, which clearly showed the greater cell inhibitory activity of these tetravalent antibodies. This markedly more potent growth-inhibiting activity with TetraMcAbs than with DiMcAbs ($P < 0.05$ for TetraMcAbs compared with their respective DiMcAbs at concentrations of 0.08, 0.4, 2, and 10 μg/mL) was also confirmed by MTT assays on the 5th day (Fig. 4*D*). Although 2F2 and C2B8 showed a similar inhibitory activity, the growth-inhibition effect of their tetravalent antibodies on lymphoma cells was significantly different. 2F2(ScFvHL)$_4$-Fc was shown to be much more effective in arresting cell growth than C2B8(ScFvHL)$_4$-Fc, yielding ~95% and ~88% inhibition of growth of Daudi and Raji cells at concentrations of 2 μg/mL and higher. Nevertheless, the maximal growth inhibition rate of the C2B8(ScFvHL)$_4$-Fc at all used concentrations on Daudi and Raji cells was ~82% and ~76%, respectively.

Pharmacokinetic properties. The pharmacokinetics of TetraMcAbs were measured in mice and compared with DiMcAbs. The pharmacokinetic variables (Table 1) indicated that C2B8 and 2F2 had similar serum half-lives *in vivo*. The $t_{1/2}$ of C2B8(ScFvHL)$_4$-Fc and 2F2(ScFvHL)$_4$-Fc was similar to that of their respective parental DiMcAbs, suggesting that the two TetraMcAbs were highly stable *in vivo*.

Therapeutic efficacy of TetraMcAbs. *In vivo* therapy studies were performed in SCID mice bearing systemic Daudi or Raji tumors. The survival curves were plotted according to Kaplan-Meier method and compared using the log-rank test. As shown in Fig. 5, when mAbs were administered to mice at a dose of 10 μg/mouse (low dose), all the four anti-CD20 mAbs, C2B8, 2F2, C2B8(ScFvHL)$_4$-Fc, and 2F2(ScFvHL)$_4$-Fc, were shown to be able to significantly improve the survival of SCID mice bearing disseminated Daudi tumor cells (SCID/Daudi; $P < 0.001$ for each compared with the PBS control). However, a pronounced difference in survival was noticed between C2B8 treatment group and either of the other three anti-CD20 mAb treatment groups ($P < 0.0001$). 2F2, C2B8(ScFvHL)$_4$-Fc, and 2F2(ScFvHL)$_4$-Fc were shown to be significantly more effective than C2B8 in prolonging the survival

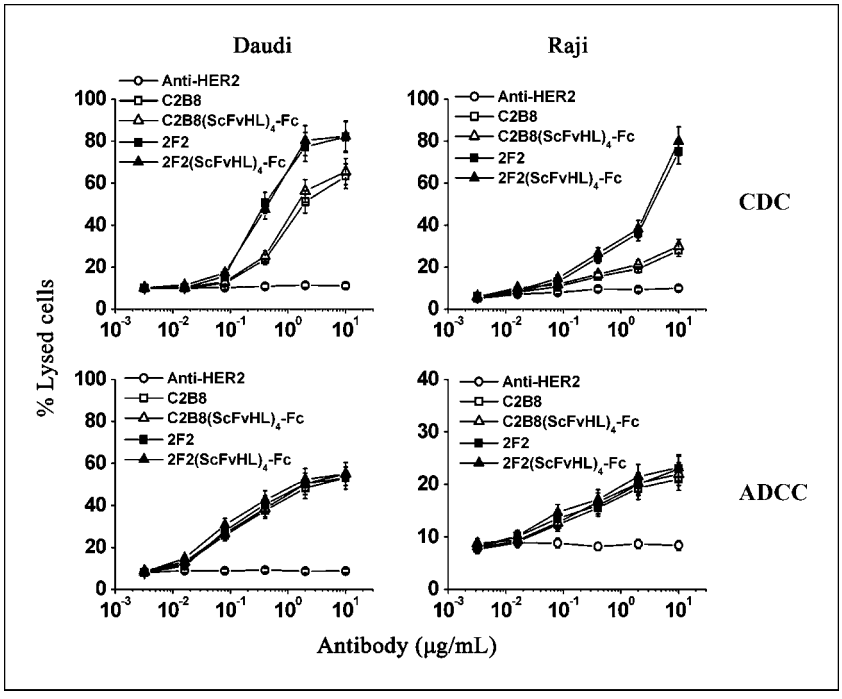

Figure 3. CDC and ADCC induced by anti-CD20 mAbs. Daudi and Raji cells were incubated with increasing concentrations of C2B8, 2F2, C2B8(ScFvHL)$_4$-Fc, or 2F2(ScFvHL)$_4$-Fc in the presence of human complement or PBMCs at 37°C for 4 h. CDC and ADCC activity of these antibodies was measured by the CytoTox 96 non-Radioactive Cytotoxicity Assay kit. Anti-HER2 is a negative control antibody. *Points,* mean ($n = 3$); *bars,* SD.

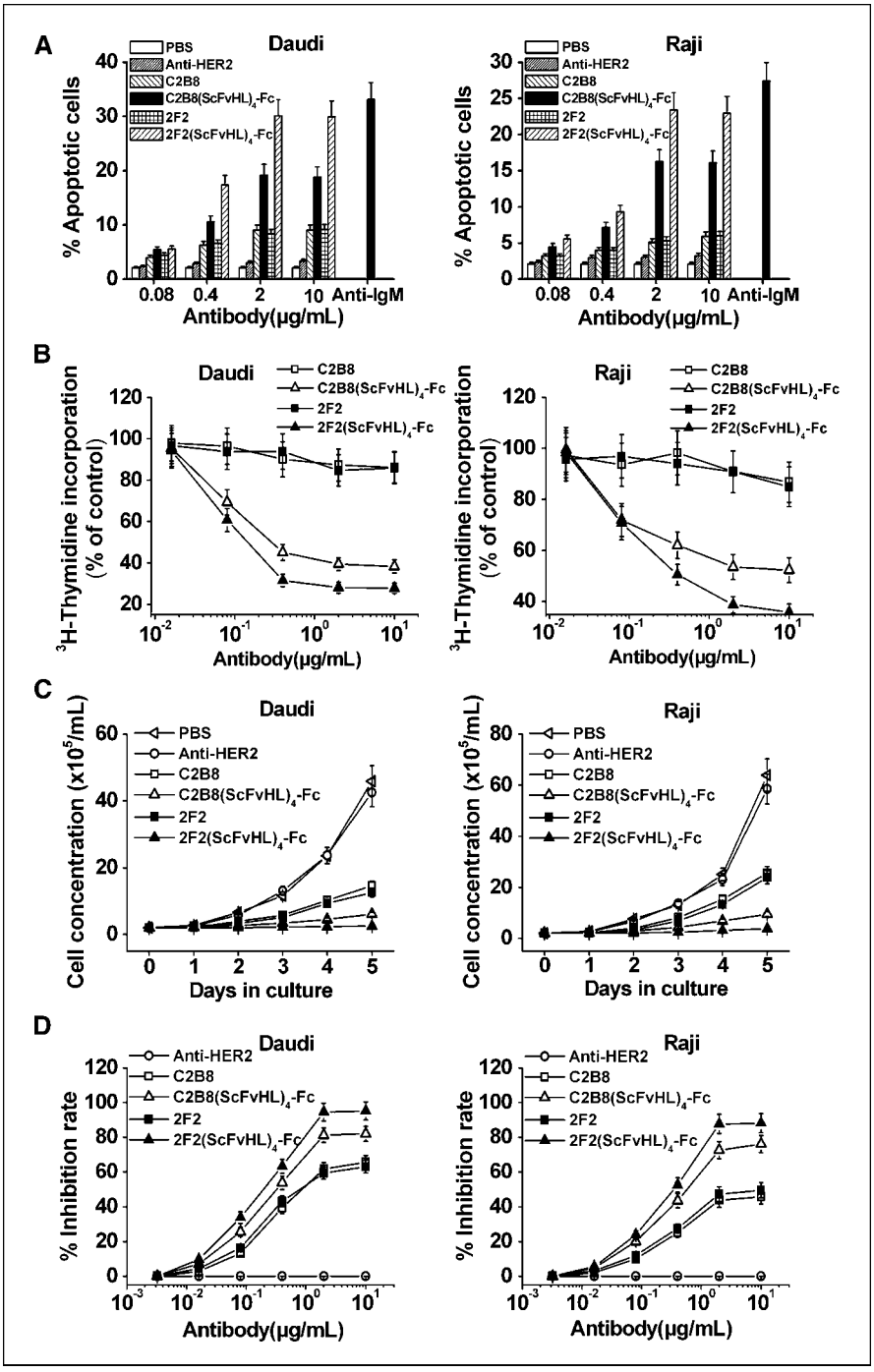

Figure 4. Antiproliferative and apoptosis-inducing activity of anti-CD20 mAbs. *A,* Apoptosis induced by anti-CD20 mAbs. Daudi or Raji cells were incubated with different concentrations of C2B8, 2F2, C2B8(ScFvHL)$_4$-Fc, or 2F2(ScFvHL)$_4$-Fc at 37°C. Apoptosis was assessed 18 h later by Annexin V staining. Apoptotic cells were measured as a percentage of total cells assayed. Anti-IgM was used as a positive control for the induction of apoptosis. Anti-HER2 is a negative control antibody. *Columns,* mean (n = 3); *bars,* SD. *B,* the effect of anti-CD20 mAbs on [^{3}H]thymidine incorporation in Daudi and Raji cells. The cells were incubated with different concentrations of C2B8, 2F2, C2B8(ScFvHL)$_4$-Fc, or 2F2(ScFvHL)$_4$-Fc at 37°C for 24 h, followed by addition of [^{3}H]thymidine. After a 12-h incubation, [^{3}H]thymidine incorporation was measured. Untreated cells were used as controls. *Points,* mean (n = 3); *bars,* SD. *C* to *D,* the inhibition of cell growth by anti-CD20 mAbs. *C,* Daudi and Raji cells were incubated with 10 μg/mL of C2B8, 2F2, C2B8(ScFvHL)$_4$-Fc, or 2F2(ScFvHL)$_4$-Fc at 37°C. Viable cells were counted daily by trypan blue exclusion for 5 d. The cell concentrations are plotted against the incubation time. *Points,* mean (n = 3); *bars,* SD. *D,* Daudi and Raji cells were treated with different concentrations of C2B8, 2F2, C2B8(ScFvHL)$_4$-Fc, or 2F2(ScFvHL)$_4$-Fc for 5 d. Then, cell growth inhibition was evaluated by MTT assays. The percentage of cell growth inhibition is presented. *Points,* mean (n = 3); *bars,* SD.

of SCID/Daudi mice. C2B8(ScFvHL)$_4$-Fc exhibited similar antitumor activity compared with that of 2F2 (P = 0.0729). It is particularly noteworthy that 2F2(ScFvHL)$_4$-Fc treatment group was significantly different from all other groups (P < 0.0001), showing a dramatic increase in survival with 40% mice alive at the termination of the experiment (day 100). Similar results were obtained using Raji cells–bearing SCID mice (SCID/Raji), which were treated with the same dose of anti-CD20 mAbs.

The results summarized in Fig. 5 also reveal that the survival of tumor-bearing mice can be prolonged by increasing the administered dose of anti-CD20 mAbs. When given at a dose of 50 μg/mouse (high dose), both C2B8(ScFvHL)$_4$-Fc and 2F2 showed a markedly improved antitumor activity compared with C2B8 [P < 0.0001 for C2B8-treated group in comparison with either the 2F2- or C2B8(ScFvHL)$_4$-Fc–treated group], but no significant difference in survival was found between C2B8(ScFvHL)$_4$-Fc and 2F2 treatment groups (P = 0.4093 for SCID/Daudi mice and P = 0.3693 for SCID/Raji mice). The animals treated with high-dose C2B8(ScFvHL)$_4$-Fc or 2F2 had similar survival curves as those treated with low-dose 2F2(ScFvHL)$_4$-Fc. However, C2B8, even when given at high dose, was shown to be much less effective in enhancing the survival of tumor-bearing mice than low-dose 2F2(ScFvHL)$_4$-Fc. 2F2(ScFvHL)$_4$-Fc seems to be far more effective than C2B8, 2F2, and C2B8(ScFvHL)$_4$-Fc [P < 0.0001 for 2F2

Table 1. Pharmacokinetics of anti-CD20 mAbs in mice

MAb	$t_{1/2}$ (h)	AUC	MRT (h)
C2B8	109.3	6,269.1	156.7
C2B8(ScFvHL)$_4$-Fc	119.5	6,438.4	169.1
2F2	101.8	5,618.3	145.6
2F2(ScFvHL)$_4$-Fc	112.3	6,451.6	161.1

Abbreviations: $t_{1/2}$, half life; AUC, area under the curve; MRT, mean residence time.

(ScFvHL)$_4$-Fc treatment group compared with either of the other three anti-CD20 mAb treatment groups], resulting in long-term survival of all mice when given at the high dose.

Discussion

In an attempt to improve anti-CD20 antibody therapeutic efficacy, we have developed two novel TetraMcAbs respectively derived from anti-CD20 DiMcAbs C2B8 and 2F2. Whereas TetraMcAb possessed four antigen-binding sites, we were unable to determine whether it used all of four binding sites to bind to the antigens. However, due to its slower off rate than DiMcAb, TetraMcAb clearly engaged more than two of its binding sites. The *in vitro* antitumor activity assays showed that TetraMcAb had antiproliferative and apoptosis-inducing activity markedly superior to that of DiMcAb. Although homodimerization of tumor-reactive monoclonal antibodies also often increases their ability to induce apoptosis and growth arrest of tumor cells, the chemically linked homodimers have several inherent disadvantages, mainly including a high molecular mass of ~300 kDa and a short half-life *in vivo* (10, 27, 28). In this study, the C2B8-derived TetraMcAb was shown to have a molecular mass of ~175 kDa, only 25 kDa higher than that of C2B8 (~150 kDa). Moreover, the results of pharmacokinetic analysis indicated that TetraMcAb was highly stable *in vivo*.

Rituximab can induce apoptosis of chronic lymphocytic leukemia cells *in vivo*, and caspase-3 activation was shown to be correlated with posttreatment lymphocyte counts (29). It has also been shown that the factors that antagonize apoptosis, such as overexpression of antiapoptotic proteins or aberrant p53 function, are associated with Rituximab resistance (30, 31). The fact that responding patients generally displayed progressive tumor mass reduction and that complete response is usually achieved several weeks after completion of therapy suggests that *in vivo* cell growth inhibition could also play an important role in the therapeutic efficacy of Rituximab (32). Our current results showed that the extent of B-lymphoma cell apoptosis induced by the various anti-CD20 mAbs decreased in the following order: 2F2(ScFvHL)$_4$-Fc > C2B8(ScFvHL)$_4$-Fc > 2F2 = C2B8. Likewise, the antiproliferative activity of these four mAbs was confirmed to be in the same descending order as indicated above. In the *in vivo* therapy studies, the two TetraMcAbs were shown to be far more effective in prolonging the survival of tumor-bearing SCID mice than their respective DiMcAbs. Because TetraMcAb displayed a similar ability to mediate CDC and ADCC against B-lymphoma cells compared with the parental DiMcAb, it could be concluded that the enhanced *in vivo* antitumor effect of TetraMcAb might be attributable to its marked increase in apoptosis-inducing and antiproliferative activity, although we were unable to discern the relative importance of the two mechanisms in contributing to improved therapeutic efficacy.

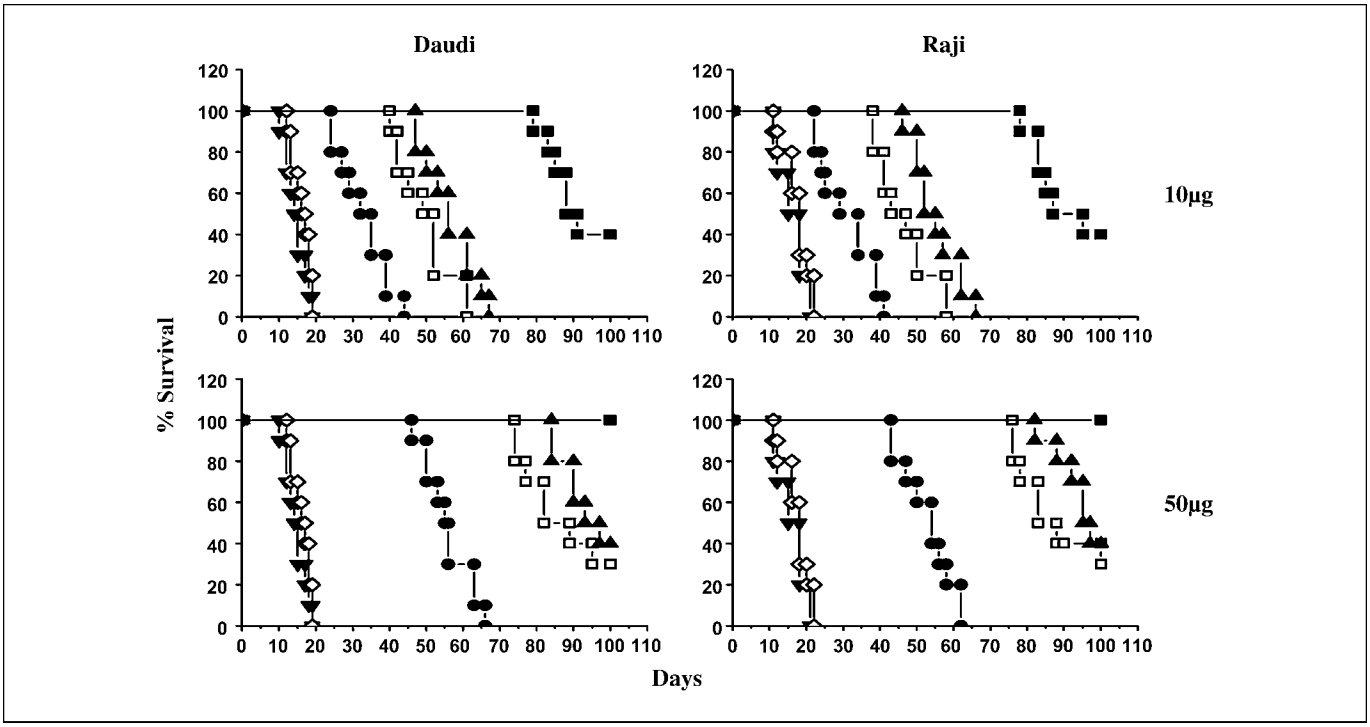

Figure 5. The survival of tumor-bearing SCID mice treated with anti-CD20 mAbs. Groups of 10 SCID mice were injected i.v. with 3.5×10^6 Raji or Daudi cells. Five days after tumor cell inoculation, the mice were treated with PBS (▼) or different doses of anti-HER2 (◇), C2B8 (●), 2F2 (□), C2B8(ScFvHL)$_4$-Fc (▲), or 2F2(ScFvHL)$_4$-Fc (■). Mice were monitored daily and sacrificed at the onset of hind leg paralysis.

The complement consumption has been observed *in vivo* after Rituximab administration, and that on some occasions, cells remaining after treatment seem to have increased levels of the complement defense molecules, consistent with the idea that they had been subject to complement selection (33–36). 2F2 is significantly more potent in CDC than C2B8 and C2B8(ScFvHL)$_4$-Fc. In the *in vivo* experimental settings, the antitumor effect of 2F2 was shown to be considerably stronger than that of C2B8, and even comparable with that of C2B8(ScFvHL)$_4$-Fc, although C2B8(ScFvHL)$_4$-Fc had antiproliferative and apoptosis-inducing activity superior to that of 2F2. These results support an important role for complement in anti-CD20 mAb immunotherapy.

In the plasma membrane, CD20 is predicted to contain two extracellular loops, a larger one between the third and fourth transmembrane regions, and a much smaller one between the first and second transmembrane regions (37, 38). Previous studies have identified the epitope recognized by Rituximab being a sequence motif (^{170}ANPS^{173}) located at the large extracellular loop (39–41). Recently, we have determined the crystal structure of the Rituximab Fab in complex with a synthesized peptide comprising the CD20 epitope at 2.6-A° resolution (42). Our structural analysis further reveals the motif ^{170}ANPS^{173} is bound at a pocket formed by four complementarity-determining region loops of the Rituximab Fab (42). Teeling et al. (38) reported that 2F2 recognized a novel epitope located N terminally of the motif ^{170}ANPS^{173}, also including the small extracellular loop of CD20. In addition, they found that one critical factor for determining the exceptionally strong CDC potency by 2F2 seemed to be the epitope it recognized. In this study, 2F2 and Rituximab were shown to equally effective in inducing cell growth arrest and apoptosis, but the functions of their TetraMcAbs were significantly different. Because TetraMcAb seemed to engage at least three of its binding sites to bind to the target molecule, whereas DiMcAb used only two, we speculated that even if there was no significant difference in antiproliferative and apoptotic activity between C2B8 and 2F2, the difference in epitopes recognized by C2B8(ScFvHL)$_4$-Fc and 2F2(ScFvHL)$_4$-Fc might account for their markedly differential ability to induce cell apoptosis or growth arrest.

Rituximab is generally well-tolerated by patients. Despite B-cell depletion, there was no increase in the incidence of infection, which had been a significant concern when Rituximab was originally investigated (43). Compared with Rituximab, 2F2(ScFvHL)$_4$-Fc has been proven to be much more effective in depleting human CD20-positive cells in the mouse model. Therefore, it is important to perform multiple preclinical toxicity studies of this new tetravalent antibody in nonhuman primates before launching clinical trials.

In conclusion, the data shown here provide further support for the idea that a combination of multiple potential mechanisms may be responsible for the therapeutic efficacy of anti-CD20 mAbs. 2F2(ScFvHL)$_4$-Fc, which not only is exceptionally active in CDC but also has surprisingly strong antiproliferative and apoptotic activity, has been shown to be an extremely potent antitumor agent in tumor-bearing mice. Currently, an evaluation of the efficacy and safety of this TetraMcAb in the cynomolgus monkey is under way.

Acknowledgments

Received 12/14/2007; revised 1/20/2008; accepted 1/21/2008.

Grant support: National Natural Science Foundation of China, Ministry of Science and Technology of China (973 and 863 program projects), and Shanghai Commission of Science and Technology.

The costs of publication of this article were defrayed in part by the payment of page charges. This article must therefore be hereby marked *advertisement* in accordance with 18 U.S.C. Section 1734 solely to indicate this fact.

We thank Yang Yang and Jing Xu for their technical assistance.

References

1. Tedder TF, Streuli M, Schlossman SF, Saito H. Isolation and structure of a cDNA encoding the B1 (CD20) cell-surface antigen of human B lymphocytes. Proc Natl Acad Sci U S A 1988;85:208–12.
2. Tedder TF, Engel P. CD20: a regulator of cell-cycle progression of B lymphocytes. Immunol Today 1994;15:450–4.
3. Maloney DG. Immunotherapy for non-Hodgkin's lymphoma: monoclonal antibodies and vaccines. J Clin Oncol 2005;23:6421–8.
4. Glennie MJ, van de Winkel JG. Renaissance of cancer therapeutic antibodies. Drug Discov Today 2003;8:503–10.
5. Leget GA, Czuczman MS. Use of rituximab, the new FDA-approved antibody. Curr Opin Oncol 1998;10:548–51.
6. Sharkey RM, Goldenberg DM. Targeted therapy of cancer: new prospects for antibodies and immunoconjugates. CA Cancer J Clin 2006;56:226–43.
7. McLaughlin P, Grillo-Lopez AJ, Link BK, et al. Rituximab chimeric anti-CD20 monoclonal antibody therapy for relapsed indolent lymphoma: half of patients respond to a four-dose treatment program. J Clin Oncol 1998;16:2825–33.
8. Maloney DG, Grillo-López AJ, Bodkin DJ, et al. IDEC-C2B8: results of a phase I multiple-dose trial in patients with relapsed non-Hodgkin's lymphoma. J Clin Oncol 1997;15:3266–74.
9. Eisenbeis CF, Caligiuri MA, Byrd JC. Rituximab: converging mechanisms of action in non-Hodgkin's lymphoma? Clin Cancer Res 2003;9:5810–2.
10. Ghetie MA, Bright H, Vitetta ES. Homodimers but not monomers of Rituxan (chimeric anti-CD20) induce apoptosis in human B-lymphoma cells and synergize with a chemotherapeutic agent and an immunotoxin. Blood 2001;97:1392–8.
11. Zhang N, Khawli LA, Hu P, Epstein AL. Generation of rituximab polymer may cause hyper-cross-linking-induced apoptosis in non-Hodgkin's lymphomas. Clin Cancer Res 2005;11:5971–80.
12. Iida S, Misaka H, Inoue M, et al. Nonfucosylated therapeutic IgG1 antibody can evade the inhibitory effect of serum immunoglobulin G on antibody-dependent cellular cytotoxicity through its high binding to FcγRIIIa. Clin Cancer Res 2006;12:2879–87.
13. Teeling JL, French RR, Cragg MS, et al. Characterization of new human CD20 monoclonal antibodies with potent cytolytic activity against non-Hodgkin lymphomas. Blood 2004;104:1793–800.
14. Nishida M, Usuda S, Okabe M, et al. Characterization of novel murine anti-CD20 monoclonal antibodies and their comparison to 2B8 and c2B8 (rituximab). Int J Oncol 2007;31:29–40.
15. Cragg MS, Morgan SM, Chan HT, et al. Complement-mediated lysis by anti-CD20 mAb correlates with segregation into lipid rafts. Blood 2003;101:1045–52.
16. Chan HT, Hughes D, French RR, et al. CD20-induced lymphoma cell death is independent of both caspases and its redistribution into triton X-100 insoluble membrane rafts. Cancer Res 2003;63:5480–89.
17. Davis T, Kamiski M, Leonard J, Gregory S. Results of a randomized study of Bexxar (Tositumomab and I 131 Tositumomab) vs unlabeled Tositumomab in patients with relapsed or refractory low-grade or transformed non-Hodgkin's lymphoma [abstract]. Blood 2001;98:843a.
18. Buchsbaum DJ, Wahl RL, Normolle DP, Kaminski MS. Therapy with unlabeled and ^{131}I-labeled pan-B-cell monoclonal antibodies in nude mice bearing Raji Burkitt's lymphoma xenografts. Cancer Res 1992;52:6476–81.
19. Reff ME, Carner K, Chambers KS, et al. Depletion of B cells *in vivo* by a chimeric mouse human monoclonal antibody to CD20. Blood 1994;83:435–45.
20. Meng R, Smallshaw JE, Pop LM, et al. The evaluation of recombinant, chimeric, tetravalent antihuman CD22 antibodies. Clin Cancer Res 2004;10:1274–81.
21. Liu XY, Pop LM, Roopenian DC, Ghetie V, Vitetta ES, Smallshaw JE. Generation and characterization of a novel tetravalent anti-CD22 antibody with improved antitumor activity and pharmacokinetics. Int Immunopharmacol 2006;6:791–9.
22. Li B, Wang H, Dai J, et al. Construction and characterization of a humanized anti-human CD3 monoclonal antibody 12F6 with effective immunoregulation functions. Immunology 2005;116:487–98.
23. Looney RJ, Abraham GN, Anderson CL. Human monocytes and U937 cells bear two distinct Fc receptors for IgG. J Immunol 1986;136:1641–7.
24. Jones DH, Looney RJ, Anderson CL. Two distinct classes of IgG Fc receptors on a human monocyte line (U937) defined by differences in binding of murine IgG subclasses at low ionic strength. J Immunol 1985;135:3348–53.
25. Mosmann T. Rapid colorimetric assay for cellular growth and survival: application to proliferation and cytotoxicity assays. J Immunol Methods 1983;65:55–63.
26. Rebello P, Hale G. Pharmacokinetics of CAMPATH-1H: assay development and validation. J Immunol Methods 2002;260:285–302.
27. Wolff EA, Schreiber GJ, Cosand WL, Raff HV. Monoclonal antibody homodimers: enhanced antitumor activity in nude mice. Cancer Res 1993;53:2560–5.

28. Ghetie MA, Podar EM, Ilgen A, Gordon BE, Uhr JW, Vitetta ES. Homodimerization of tumor-reactive monoclonal antibodies markedly increases their ability to induce growth arrest or apoptosis of tumor cells. Proc Natl Acad Sci U S A 1997;94:7509–14.

29. Clark EA, Ledbetter JA. How does B cell depletion therapy work, and how can it be improved? Ann Rheum Dis 2005;64:77–80.

30. Bannerji R, Kitada S, Flinn IW, et al. Apoptotic-regulatory and complement-protecting protein expression in chronic lymphocytic leukemia: relationship to *in vivo* rituximab resistance. J Clin Oncol 2003;21:1466–71.

31. Byrd JC, Smith L, Hackbarth ML, et al. Interphase cytogenetic abnormalities in chronic lymphocytic leukemia may predict response to rituximab. Cancer Res 2003;63:36–8.

32. Bezombes C, Grazide S, Garret C, et al. Rituximab antiproliferative effect in B-lymphoma cells is associated with acid-sphingomyelinase activation in raft microdomains. Blood 2004;104:1166–73.

33. van der Kolk LE, Grillo-Lopez AJ, Baars JW, Hack CE, van Oers MH. Complement activation plays a key role in the side-effects of rituximab treatment. Br J Haematol 2001;115:807–11.

34. Winkler U, Jensen M, Manzke O, Schulz H, Diehl V, Engert A. Cytokine-release syndrome in patients with B-cell chronic lymphocytic leukemia and high lymphocyte counts after treatment with an anti-CD20 monoclonal antibody (rituximab, IDEC-C2B8). Blood 1999;94:2217–24.

35. Treon SP, Mitsiades C, Mitsiades N, et al. Tumor cell expression of CD59 is associated with resistance to CD20 serotherapy in patients with B-cell malignancies. J Immunother 2001;24:263–71.

36. Bannerji RPM, Flinn IW. Cell surface complement inhibitors CD55 and CD59 may mediate chronic lymphocytic leukemia (CLL) resistance to rituximab therapy [abstract]. Blood 2000;96:164.

37. Polyak MJ, Tailor SH, Deans JP. Identification of a cytoplasmic region of CD20 required for its redistribution to a detergent-insoluble membrane compartment. J Immunol 1998;161:3242–8.

38. Teeling JL, Mackus WJ, Wiegman LJ, et al. The biological activity of human CD20 monoclonal antibodies is linked to unique epitopes on CD20. J Immunol 2006;177:362–71.

39. Polyak MJ, Deans JP. Alanine-170 and proline-172 are critical determinants for extracellular CD20 epitopes;heterogeneity in the fine specificity of CD20 monoclonal antibodies is defined by additional requirements imposed by both amino acid sequence and quaternary structure. Blood 2002;99:3256–62.

40. Perosa F, Favoino E, Caragnano MA, Dammacco F. Generation of biologically active linear and cyclic peptides has revealed a unique fine specificity of rituximab and its possible cross-reactivity with acid sphingomyelinase-like phosphodiesterase 3b precursor. Blood 2006;107:1070–7.

41. Binder M, Otto F, Mertelsmann R, Veelken H, Trepel M. The epitope recognized by rituximab. Blood 2006;108:1975–8.

42. Du J, Wang H, Zhong C, et al. Structural basis for recognition of CD20 by therapeutic antibody Rituximab. J Biol Chem 2007;282:15073–80.

43. Mohrbacher A. B cell non-Hodgkin's lymphoma: rituximab safety experience. Arthritis Res Ther 2005;7 Suppl 3:S19–25.